

Multi-Branch Tensor Network Structure for Tensor-Train Discriminant Analysis

Seyyid Emre Sofuoğlu, Selin Aviyente

Abstract—Higher-order data with high dimensionality arise in a diverse set of application areas such as computer vision, video analytics and medical imaging. Tensors provide a natural tool for representing these types of data. Although there has been a lot of work in the area of tensor decomposition and low-rank tensor approximation, extensions to supervised learning, feature extraction and classification are still limited. Moreover, most of the existing supervised tensor learning approaches are based on the orthogonal Tucker model. However, this model has some limitations for large tensors including high memory and computational costs. In this paper, we introduce a supervised learning approach for tensor classification based on the tensor-train model. In particular, we introduce a multi-branch tensor network structure for efficient implementation of tensor-train discriminant analysis (TTDA). The proposed approach takes advantage of the flexibility of the tensor train structure to implement various computationally efficient versions of TTDA. This approach is then evaluated on image and video classification tasks with respect to computation time, storage cost and classification accuracy and is compared to both vector and tensor based discriminant analysis methods.

Index terms— Tensor-Train, Tensor Networks, Multidimensional Discriminant Analysis, Supervised Tensor-Train.

I. INTRODUCTION

Tensors, which are higher order generalizations of matrices and vectors, provide a natural way to represent multi-dimensional data objects whose entries are indexed by several continuous or discrete variables. Employing tensors and their decompositions to process data objects has become increasingly popular [1], [2], [3]. For instance, a color image is a third-order tensor defined by two indices for spatial variables and one index for color mode. A video comprised of color images is a fourth-order tensor with an additional index for the time variable. Majority of the current work on tensor decomposition is focused on unsupervised learning of low-rank representations of the tensor object, e.g. PARAFAC [4] and Tucker decomposition [5], [3], [6], [7].

In many real-world applications such as computer vision, data instances are more naturally represented as second-order or higher-order tensors, where the order of a tensor corresponds to the number of modes. Conventional supervised learning approaches including LDA applied to vectorized tensor samples are inadequate when dealing with massive multidimensional data as they cannot capture the cross-couplings across the different modes and suffer from increasing storage

and computational costs [2], [8], [1]. Therefore, there is a growing need for new methods that account for the intrinsic structure of data while learning discriminant subspaces.

In recent years, supervised and unsupervised tensor subspace learning approaches based on the Tucker model have been proposed [9], [10], [11], [12], [13]. Some of these approaches such as Multilinear Principal Component Analysis (MPCA) [13] is successful at dimensionality reduction but is not necessarily suitable for discriminative feature extraction. Others such as Multilinear Discriminant Analysis (MDA) [9] are not practical with increasing number of modes, due to exponential increase in the storage cost of Tucker model [14].

Tensor-Train (TT) model, on the other hand, provides better compression than Tucker models, especially for higher order tensors, as it expresses a given high-dimensional tensor as the product of low-rank, 3-mode tensors [2]. TT model has been employed in various applications such as PCA [15], manifold learning [16] and deep learning [17]. In this paper, we introduce a discriminant subspace learning approach using the TT model, namely the Tensor-Train Discriminant Analysis (TTDA). The proposed approach is based on the linear discriminant analysis (LDA) and approximates the LDA subspace by putting a constraint such that it has a TT structure. Although this constraint provides an efficient structure for storing the learned subspaces, it is computationally prohibitive. For this reason, we propose several computationally efficient implementations of TTDA utilizing the flexibility of the tensor network structure. Previous work on TT and tensor networks in general, brings up the question of whether reshaping high-dimensional vector- and matrix-type data into tensors and then processing them using TT decomposition provides any significant benefits [18]. Several papers employed this idea to reshape matrices into tensors, known as ket augmentation and quantized TT (QTT), for better compression and higher computational efficiency [19], [16], [18], [20]. In QTT, a vector or a matrix is tensorized to a higher order tensor to improve both the computational complexity and storage cost of TT. Inspired by this idea, we propose to tensorize the projected training samples in a learning framework. Once the projections are tensorized, the corresponding TT subspaces become smaller in dimension. Using this structural approximation to TTDA, first we propose approximating 2D-LDA by TT and then generalize by increasing the number of modes (or branches) of the projected training samples.

This paper differs from current work in two ways. First, we generalize discriminant analysis using TT model, and propose several approaches to implement this generalization using the efficiency of multi-branch Tensor Network structure

This work was in part supported by NSF CCF-1615489.

S. E. Sofuoğlu and S. Aviyente are with Electrical and Computer Engineering, Michigan State University, East Lansing, MI, 48824, USA. E-mails: sofuoğlu@msu.edu, aviyente@egr.msu.edu

in discriminant analysis. Second, we explore computational and storage complexity in terms of the number of modes of the projection tensors. Therefore, depending on the input tensor dimensions, we provide a method to find the most efficient way to implement the TT model.

The rest of the paper is organized as follows. In Section II, we provide background on tensor operations, TT and Tucker decomposition, LDA and MDA. In Section III, we propose several approaches to implement tensor-train discriminant analysis. We also provide storage cost and computational complexities for the proposed approaches and propose an optimal structure for decomposing a given tensor object in terms of storage complexity. In Section IV, we compare the proposed methods with state-of-the-art tensor based discriminant analysis methods for classification applications.

II. BACKGROUND

Let $\mathcal{Y} \in \mathbb{R}^{I_1 \times \dots \times I_N \times K \times C}$ be the collection of tensor training data samples. Define $\mathcal{Y}_c^k \in \mathbb{R}^{I_1 \times I_2 \times \dots \times I_N}$ as the sample tensors where $c \in \{1, \dots, C\}$ is the class index and $k \in \{1, \dots, K\}$ is the sample index, from a given \mathcal{Y} with C classes where each class has K samples.

A. Notation

Definition 1. (Vectorization, Matricization and Reshaping) $\mathbf{V}(\cdot)$ is a vectorization operator such that $\mathbf{V}(\mathcal{Y}_c^k) \in \mathbb{R}^{I_1 I_2 \dots I_N \times 1}$. $\mathbf{T}_n(\cdot)$ is a tensor-to-matrix reshaping operator defined as $\mathbf{T}_n(\mathcal{Y}_c^k) \in \mathbb{R}^{I_1 \dots I_n \times I_{n+1} \dots I_N}$ and the inverse operator is denoted as $\mathbf{T}_n^{-1}(\cdot)$.

Definition 2. (Left and right unfolding) The left unfolding operator creates a matrix from a tensor by taking all modes except the last mode as row indices and the last mode as column indices, i.e. $\mathbf{L}(\mathcal{Y}_c^k) \in \mathbb{R}^{I_1 I_2 \dots I_{N-1} \times I_N}$ which is equivalent to $\mathbf{T}_{N-1}(\mathcal{Y}_c^k)$. Right unfolding transforms a tensor to a matrix by taking all the first mode fibers as column vectors, i.e. $\mathbf{R}(\mathcal{Y}_c^k) \in \mathbb{R}^{I_1 \times I_2 I_3 \dots I_N}$ which is equivalent to $\mathbf{T}_1(\mathcal{Y}_c^k)$. The inverse of these operators are denoted as $\mathbf{L}^{-1}(\cdot)$ and $\mathbf{R}^{-1}(\cdot)$, respectively.

Definition 3. (Tensor trace) Tensor trace is applied on matrix slices of a tensor and contracts the matrices to a scalar. Let $\mathcal{A} \in \mathbb{R}^{I_1 \times I_2 \times \dots \times I_N}$ with $I_1 = I_k$, then trace operation on modes 1 and k is defined as:

$$\mathcal{D} = \text{tr}_1^k(\mathcal{A}) = \sum_{i_1=i_k=1}^{I_1} \mathcal{A}(i_1, :, \dots, i_k, :, \dots, :), \quad (1)$$

where $\mathcal{D} \in \mathbb{R}^{I_2 \times I_4 \times I_5 \times \dots \times I_N}$ is a $N-2$ -mode tensor.

Definition 4. (Tensor Merging Product) Tensor merging product connects two tensors along some given sets of modes. For two tensors $\mathcal{A} \in \mathbb{R}^{I_1 \times I_2 \times \dots \times I_N}$ and $\mathcal{B} \in \mathbb{R}^{J_1 \times J_2 \times \dots \times J_M}$ where $I_n = J_m$ and $I_{n+1} = J_{m-1}$ for some n and m , tensor merging product is given by [14]:

$$\mathcal{C} = \mathcal{A} \times_{n, n+1}^{m, m-1} \mathcal{B}. \quad (2)$$

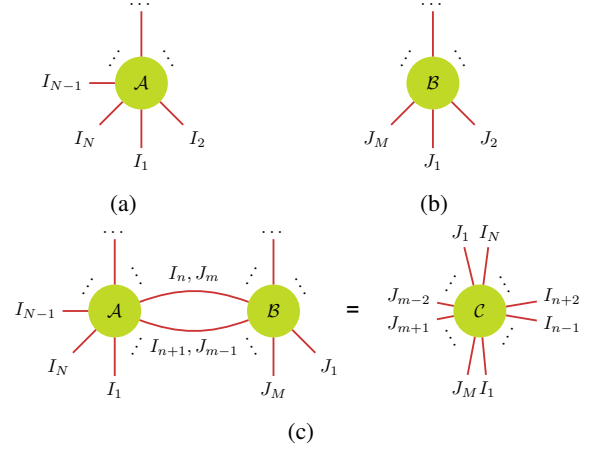


Fig. 1: Illustration of tensors and tensor merging product using tensor network notations. Each node represents a tensor and each edge represents a mode of the tensor. (a) Tensor \mathcal{A} , (b) Tensor \mathcal{B} , (c) Tensor Merging Product between modes (n, m) and $(n+1, m-1)$.

$\mathcal{C} \in \mathbb{R}^{I_1 \times \dots \times I_{n-1} \times I_{n+2} \times \dots \times I_N \times J_1 \times \dots \times J_{m-2} \times J_{m+1} \times \dots \times J_M}$ is a $(N+M-4)$ -mode tensor that is calculated as:

$$\begin{aligned} \mathcal{C}(i_1, \dots, i_{n-1}, i_{n+2}, \dots, i_N, j_1, \dots, j_{m-2}, j_{m+1}, \dots, j_M) = \\ \sum_{t_1=1}^{I_n} \sum_{t_2=1}^{J_{m-1}} [\mathcal{A}(i_1, \dots, i_{n-1}, i_n = t_1, i_{n+1} = t_2, i_{n+1}, \dots, i_N) \\ \mathcal{B}(j_1, \dots, j_{m-2}, j_{m-1} = t_2, j_m = t_1, j_{m+1}, \dots, j_M)]. \quad (3) \end{aligned}$$

A graphical representation of tensors \mathcal{A} and \mathcal{B} and tensor merging product above is given in Fig. 1.

A special case of the tensor merging product can be considered for the case where $I_n = J_m$ for all $n, m \in \{1, \dots, N-1\}, M \geq N$. In this case, the tensor merging product across the first $N-1$ modes is defined as:

$$\mathcal{C}' = \mathcal{A} \times_{1, \dots, N-1}^{1, \dots, N-1} \mathcal{B}, \quad (4)$$

where $\mathcal{C}' \in \mathbb{R}^{I_N \times J_N \times \dots \times J_M}$. This can equivalently be written as:

$$\mathbf{R}(\mathcal{C}') = \mathbf{L}(\mathcal{A})^\top \mathbf{T}_{N-1}(\mathcal{B}), \quad (5)$$

where $\mathbf{R}(\mathcal{C}') \in \mathbb{R}^{I_N \times \prod_{m=N}^M J_m}$.

Definition 5. (Tensor Train Decomposition (TT Decomposition)) Using tensor-train decomposition, each element of \mathcal{Y}_c^k can be represented as:

$$\begin{aligned} \mathcal{Y}_c^k(i_1, i_2, \dots, i_N) = \\ \mathcal{U}_1(1, i_1, :) \mathcal{U}_2(:, i_2, :) \dots \mathcal{U}_N(:, i_N, :) \mathbf{x}_c^k, \quad (6) \end{aligned}$$

where $\mathcal{U}_n \in \mathbb{R}^{R_{n-1} \times I_n \times R_n}$ are the three mode low-rank tensor factors, $R_n < I_n$ are the TT-ranks of the corresponding modes $n \in \{1, \dots, N\}$ and $\mathbf{x}_c^k \in \mathbb{R}^{R_N \times 1}$ is the projected sample vector. Using tensor merging product form, (6) can be rewritten as

$$\mathcal{Y}_c^k = \mathcal{U}_1 \times_3^1 \mathcal{U}_2 \times_3^1 \dots \times_3^1 \mathcal{U}_N \times_3^1 \mathbf{x}_c^k. \quad (7)$$

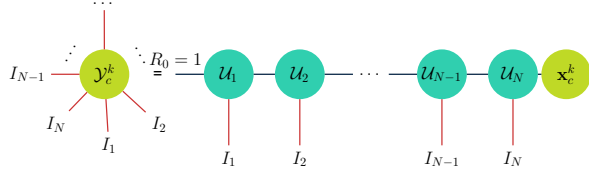


Fig. 2: Tensor Train Decomposition of \mathcal{Y}_c^k using tensor merging products.

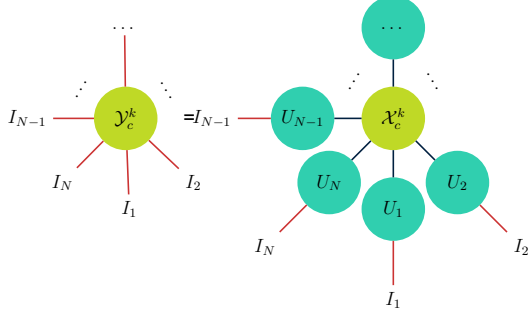


Fig. 3: Tensor network notation for Tucker decomposition.

A graphical representation of (7) can be seen in Fig. 2. If \mathcal{Y}_c^k is vectorized, another equivalent expression for (6) in terms of matrix projection is obtained as:

$$\mathbf{V}(\mathcal{Y}_c^k) = \mathbf{L}(U_1 \times_3 U_2 \times_3 \cdots \times_3 U_N) \mathbf{x}_c^k. \quad (8)$$

For the sake of simplicity, we define $U = \mathbf{L}(U_1 \times_3 U_2 \times_3 \cdots \times_3 U_N)$ where $U \in \mathbb{R}^{I_1 I_2 \cdots I_N \times R_N}$. When $\mathbf{L}(U_n)$ s are left orthogonal, U is also left orthogonal [21], i.e. $\mathbf{L}(U_n)^\top \mathbf{L}(U_n) = \mathbb{I}_{R_{n-1} I_n}, \forall n$ leads to $U^\top U = \mathbb{I}_I, I = \prod_{n=1}^N I_n$ where \mathbb{I}_c is defined as the identity matrix with size $c \times c$.

Definition 6. (Tucker Decomposition (TD)) If the number of modes of the projected samples \mathcal{X}_c^k is equal to the number of modes of the input tensors \mathcal{Y}_c^k , the TT-model becomes equivalent to Tucker decomposition. In this case, \mathcal{X}_c^k is also known as the core tensor. This is given in (9) and also shown in Fig. 3:

$$\mathcal{Y}_c^k = \mathcal{X}_c^k \times_1^2 U_1 \times_2^2 U_2 \cdots \times_N^2 U_N, \quad (9)$$

where $U_n \in \mathbb{R}^{I_n \times R_n}$ and $\mathcal{X}_c^k \in \mathbb{R}^{R_1 \times R_2 \times \cdots \times R_N}$.

B. Linear Discriminant Analysis (LDA)

LDA for vectorized tensor data finds an orthogonal projection U that maximizes the discriminability of projections:

$$U = \underset{\hat{U}}{\operatorname{argmin}} \left[\operatorname{tr}(\hat{U}^\top S_W \hat{U}) - \lambda \operatorname{tr}(\hat{U}^\top S_B \hat{U}) \right] = \underset{\hat{U}}{\operatorname{argmin}} \operatorname{tr}(\hat{U}^\top (S_W - \lambda S_B) \hat{U}) = \underset{\hat{U}}{\operatorname{argmin}} \operatorname{tr}(\hat{U}^\top S \hat{U}), \quad (10)$$

where $S = S_W - \lambda S_B$, λ is the regularization parameter that controls the trade-off between S_W and S_B which are within-

class and between-class scatter matrices, respectively, given by:

$$S_W = \sum_{c=1}^C \sum_{k=1}^K \mathbf{V}(\mathcal{Y}_c^k - \mathcal{M}_c) \mathbf{V}(\mathcal{Y}_c^k - \mathcal{M}_c)^\top, \quad (11)$$

$$S_B = \sum_{c=1}^C \sum_{k=1}^K \mathbf{V}(\mathcal{M}_c - \mathcal{M}) \mathbf{V}(\mathcal{M}_c - \mathcal{M})^\top, \quad (12)$$

where $\mathcal{M}_c = \frac{1}{K} \sum_{k=1}^K \mathcal{Y}_c^k$ is the sample mean for each class c and $\mathcal{M} = \frac{1}{CK} \sum_{c=1}^C \sum_{k=1}^K \mathcal{Y}_c^k$ is the total mean of all sample tensors. Since U is an orthogonal projection matrix, (10) is equivalent to minimizing the within-class scatter and maximizing the between class scatter of projections, which can be solved by taking the eigenvectors corresponding to the lowest R_N eigenvalues of $S \in \mathbb{R}^{\prod_{n=1}^N I_n \times \prod_{n=1}^N I_n}$ as U , i.e. $U \in \mathbb{R}^{\prod_{n=1}^N I_n \times R_N}$.

C. Multilinear Discriminant Analysis (MDA)

MDA extends TD to supervised learning by finding a subspace $U_n \in \mathbb{R}^{I_n \times R_n}$ for each mode $n \in \{1, \dots, N\}$ that maximizes the discriminability along that mode [10], [11], [9]. When the number of modes N is 1, MDA is equivalent to LDA. In the case of MDA, within-class scatter along each mode $n \in \{1, \dots, N\}$ is defined as:

$$S_W^{(n)} = \sum_{c=1}^C \sum_{k=1}^{K_c} \left[(\mathcal{Y}_c^k - \mathcal{M}_c) \prod_{\substack{m \in \{1, \dots, N\} \\ m \neq n}} \times_m^1 U_m \right]_{(n)} \left[(\mathcal{Y}_c^k - \mathcal{M}_c) \prod_{\substack{m \in \{1, \dots, N\} \\ m \neq n}} \times_m^1 U_m \right]_{(n)}^\top. \quad (13)$$

Between-class scatter $S_B^{(n)}$ is also found in a similar manner. Using these definitions of the scatter matrices, each U_n is found by optimizing [11]:

$$U_n = \underset{\hat{U}_n}{\operatorname{argmin}} \operatorname{tr}(\hat{U}_n^\top (S_W^{(n)} - \lambda S_B^{(n)}) \hat{U}_n). \quad (14)$$

Different implementations of the multiway discriminant analysis have been introduced including Discriminant Analysis with Tensor Representation (DATER), Direct Generalized Tensor Discriminant Analysis (DGTDA) and Constrained MDA (CMDA). DATER minimizes the ratio $\operatorname{tr}(U_n^\top S_W^{(n)} U_n) / \operatorname{tr}(U_n^\top S_B^{(n)} U_n)$ [10]. Direct Generalized Tensor Discriminant Analysis (DGTDA), on the other hand, finds the solution for each mode independent of the other modes, i.e. computes scatter matrices without projecting inputs on U_m , where $m \neq n$ for each mode n and updates U_n using these [9]. Constrained MDA (CMDA) finds the solution in an iterative fashion [9], where each subspace is found by fixing all other subspaces. As these approaches use Tucker Decomposition, their storage complexity becomes inefficient with increasing number of modes and samples. In this paper, we propose using novel TT-based models to overcome this problem while still having similar or better computational complexity.

III. METHODS FOR TENSOR-TRAIN DISCRIMINANT ANALYSIS

When the data are higher order tensors, LDA needs to first vectorize them and then find an optimal projection as shown in (10). This creates several problems as the intrinsic structure of the data is destroyed and dimensionality, computation time and storage cost increase exponentially. Thus, in this section we propose to solve the above problem by constraining $U = \mathbf{L}(\mathcal{U}_1 \times_3 \mathcal{U}_2 \times_3 \dots \times_3 \mathcal{U}_N)$ to be a TT subspace to reduce the computational and storage complexity and to obtain a solution that will preserve the inherent structure. With this approach, the obtained U will still result in discriminative features and will have additional structure imposed by the TT.

A. TT Discriminant Analysis (TTDA):

The goal of TTDA is to learn left orthogonal tensor factors $\mathcal{U}_n \in \mathbb{R}^{R_{n-1} \times I_n \times R_n}$, $n \in \{1, \dots, N\}$ using TT-model such that the discriminability of projections \mathbf{x}_c^k , $\forall c, k$ is maximized. Using TT decomposition proposed in [22] $\mathcal{U}_n, \forall n$ can be initialized. To optimize \mathcal{U}_n s for discriminability, we need to solve (10) for each \mathcal{U}_n , which can be rewritten using the definition of U as:

$$\mathcal{U}_n = \underset{\hat{\mathcal{U}}_n}{\operatorname{argmin}} \operatorname{tr} \left[\mathbf{L}(\mathcal{U}_1 \times_3 \dots \times_3 \hat{\mathcal{U}}_n \times_3 \dots \times_3 \mathcal{U}_N)^\top \mathbf{S} \mathbf{L}(\mathcal{U}_1 \times_3 \dots \times_3 \hat{\mathcal{U}}_n \times_3 \dots \times_3 \mathcal{U}_N) \right]. \quad (15)$$

Using the definitions presented in (4) and (5), we can express (15) in terms of tensor merging product:

$$\mathcal{U}_n = \underset{\hat{\mathcal{U}}_n}{\operatorname{argmin}} \operatorname{tr} \left[(\mathcal{U}_1 \times_3 \dots \times_3 \mathcal{U}_N) \times_{1, \dots, N}^{\mathcal{S}} \times_{N+1, \dots, 2N}^{\mathcal{U}_1 \times_3 \dots \times_3 \mathcal{U}_N} \right], \quad (16)$$

where $\mathcal{S} = \mathbf{T}_N^{-1}(\mathcal{S}) \in \mathbb{R}^{I_1 \times \dots \times I_N \times I_1 \times \dots \times I_N}$. Let $\mathcal{U}_{n-1}^L = \mathcal{U}_1 \times_3 \mathcal{U}_2 \times_3 \dots \times_3 \mathcal{U}_{n-1}$ and $\mathcal{U}_n^R = \mathcal{U}_{n+1} \times_3 \dots \times_3 \mathcal{U}_N$. By rearranging the terms in (16), we can first compute all merging products and trace operations that do not involve \mathcal{U}_n and then write the optimization problem only in terms of \mathcal{U}_n . Thus, we first define:

$$\mathcal{A}_n = \operatorname{tr}_4^8 \left[\mathcal{U}_{n-1}^L \times_{1, \dots, n-1}^{1, \dots, n-1} \left(\mathcal{U}_n^R \times_{1, \dots, N-n}^{n+1, \dots, N} \mathcal{S} \right) \right], \quad (17)$$

where $\mathcal{A}_n \in \mathbb{R}^{R_{n-1} \times I_n \times R_n \times R_{n-1} \times I_n \times R_n}$ (refer to Fig. 4 for a graphical representation of (17)). Then, (15) is equivalent to:

$$\mathcal{U}_n = \underset{\hat{\mathcal{U}}_n}{\operatorname{argmin}} \left(\hat{\mathcal{U}}_n \times_{1,2,3}^{1,2,3} \left(\mathcal{A}_n \times_{4,5,6}^{1,2,3} \hat{\mathcal{U}}_n \right) \right). \quad (18)$$

Let $A_n = \mathbf{T}_3(\mathcal{A}_n) \in \mathbb{R}^{R_{n-1} I_n R_n \times R_{n-1} I_n R_n}$, then (18) can be rewritten as:

$$\mathcal{U}_n = \underset{\hat{\mathcal{U}}_n}{\operatorname{argmin}} \mathbf{V}(\hat{\mathcal{U}}_n)^\top A_n \mathbf{V}(\hat{\mathcal{U}}_n), \quad \mathbf{L}(\hat{\mathcal{U}}_n)^\top \mathbf{L}(\hat{\mathcal{U}}_n) = \mathbb{I}_{R_{n-1} I_n}. \quad (19)$$

This is a convex function with unitary constraints and can be solved by the algorithm proposed in [23]. The procedure described above to find the subspaces is computationally expensive and takes a long time to solve due to the complexity of finding each \mathcal{A}_n [16].

When $n = N$, (19) does not apply as \mathcal{U}_N^R is not defined and the trace operation is defined on the third mode of \mathcal{U}_N . To update \mathcal{U}_N , the following can be used:

$$\mathcal{U}_N = \underset{\hat{\mathcal{U}}_N}{\operatorname{argmin}} \operatorname{tr} \left(\hat{\mathcal{U}}_N \times_{1,2}^{1,2} \left(\mathcal{A}_N \times_{3,4}^{1,2} \hat{\mathcal{U}}_N \right) \right), \quad (20)$$

where $\mathcal{A}_N = \mathcal{U}_{N-1}^L \times_{1, \dots, N-1}^{1, \dots, N-1} \left(\mathcal{U}_{N-1}^L \times_{1, \dots, N-1}^{N+1, \dots, 2N-1} \mathcal{S} \right)$. See Fig. 5 for a graphical representation of \mathcal{A}_N . The pseudocode for TTDA is given in Algorithm 1.

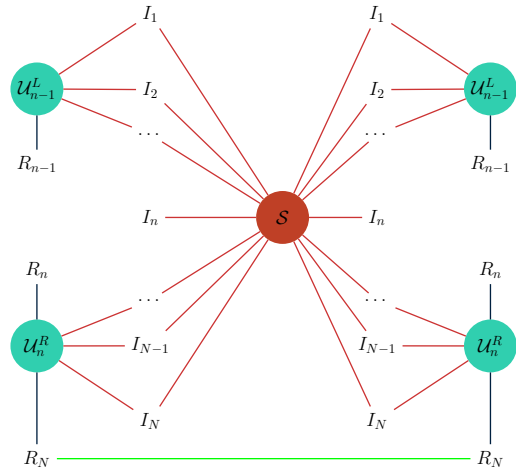


Fig. 4: Tensor \mathcal{A}_n formed by merging \mathcal{U}_n^R , \mathcal{U}_{n-1}^L and \mathcal{S} , then applying trace on 4th and 8th modes. Green line indicates tensor trace operation.

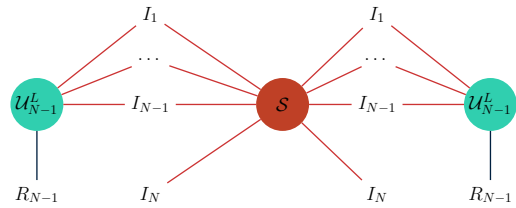


Fig. 5: Tensor \mathcal{A}_N is different from all other \mathcal{A}_n s as the trace operation is on the third mode of \mathcal{U}_N and \mathcal{U}_N^R is not defined.

B. Two-way Tensor Train Discriminant Analysis (2WTTDA):

As LDA tries to find a subspace U which maximizes discriminability for vector-type data, similarly 2D-LDA tries to find two subspaces V_1, V_2 such that these subspaces maximize discriminability for matrix-type data [24]. If one considers the matricized version of \mathcal{Y}_c^k along mode d , i.e. $\mathbf{T}_d(\mathcal{Y}_c^k) \in \mathbb{R}^{\prod_{i=1}^d I_i \times \prod_{i=d+1}^N I_i}$, where $1 < d < N$, the equivalent orthogonal projection can be written as:

$$\mathbf{T}_d(\mathcal{Y}_c^k) = V_1 X_c^k V_2^\top, \quad (21)$$

Algorithm 1 Tensor-Train Discriminant Analysis (TTDA)

Input: Input tensors $\mathcal{Y}_c^k \in \mathbb{R}^{I_1 \times I_2 \times \dots \times I_N}$ where $c \in \{1, \dots, C\}$ and $k \in \{1, \dots, K\}$, initial tensor factors $\mathcal{U}_n, n \in \{1, \dots, N\}$, $\lambda, R_1, \dots, R_N, MaxIter$

Output: $\mathcal{U}_n, n \in \{1, \dots, N\}$, and $\mathbf{x}_c^k, \forall c, k$

- 1: $\mathcal{S} \leftarrow \mathbf{T}_N^{-1}(S_W - \lambda S_B)$, see eqns.(11), (12).
 - 2: **while** $iter < MaxIter$ **do**
 - 3: **for** $n = 1 : N - 1$ **do**
 - 4: $\mathcal{A}_n \leftarrow tr_4^s \left[\mathcal{U}_{n-1}^L \times_{1, \dots, n-1}^{1, \dots, n-1} \left(\mathcal{U}_n^R \times_{1, \dots, N-n}^{n+1, \dots, N} \left(\mathcal{U}_{n-1}^L \times_{1, \dots, n-1}^{N+1, \dots, N+n-1} \left(\mathcal{U}_n^R \times_{1, \dots, N-n}^{N+n+1, \dots, 2N} \mathcal{S} \right) \right) \right) \right]$.
 - 5: $\mathbf{V}(\mathcal{U}_n) = \operatorname{argmin}_{\hat{\mathcal{U}}_n} \mathbf{V}(\hat{\mathcal{U}}_n)^\top \mathbf{T}_3(\mathcal{A}_n) \mathbf{V}(\hat{\mathcal{U}}_n)$.
 - 6: **end for**
 - 7: $\mathcal{A}_N \leftarrow \mathcal{U}_{N-1}^L \times_{1, \dots, N-1}^{1, \dots, N-1} \left(\mathcal{U}_N^L \times_{1, \dots, N-1}^{N+1, \dots, 2N-1} \mathcal{S} \right)$.
 - 8: $\mathbf{L}(\mathcal{U}_N) \leftarrow \operatorname{argmin}_{\hat{\mathcal{U}}_N} tr \left(\mathbf{L}(\hat{\mathcal{U}}_N)^\top \mathbf{T}_2(\mathcal{A}_N) \mathbf{L}(\hat{\mathcal{U}}_N) \right)$.
 - 9: $iter \leftarrow iter + 1$.
 - 10: **end while**
 - 11: $U = \mathbf{L}(\mathcal{U}_1 \times_{\frac{1}{3}} \mathcal{U}_2 \times_{\frac{1}{3}} \dots \times_{\frac{1}{3}} \mathcal{U}_N)$
 - 12: $\mathbf{x}_c^k \leftarrow U^\top \mathbf{V}(\mathcal{Y}_c^k), \forall c, k$.
-

where $V_1 \in \mathbb{R}^{\prod_{i=1}^d I_i \times R_d}, V_2 \in \mathbb{R}^{\prod_{i=d+1}^N I_i \times \hat{R}_d}$ and $X_c^k \in \mathbb{R}^{R_d \times \hat{R}_d}$.

In TTDA, since the projections \mathbf{x}_c^k are considered to be vectors, the subspace $U = \mathbf{L}(\mathcal{U}_1 \times_{\frac{1}{3}} \mathcal{U}_2 \times_{\frac{1}{3}} \dots \times_{\frac{1}{3}} \mathcal{U}_N)$ is analogous to the solution of LDA with the constraint that the subspace admits a TT model. If we consider the projections and the input samples as matrices, now we can impose a TT structure to the two subspaces (left and right subspaces) analogous to 2D-LDA, instead of LDA. In other words, one can find two sets of TT representations corresponding to V_1 and V_2 in (21). Using this analogy, (21) can be rewritten as:

$$\mathbf{T}_d(\mathcal{Y}_c^k) = \mathbf{L}(\mathcal{U}_1 \times_{\frac{1}{3}} \dots \times_{\frac{1}{3}} \mathcal{U}_d) X_c^k \mathbf{R}(\mathcal{U}_{d+1} \times_{\frac{1}{3}} \dots \times_{\frac{1}{3}} \mathcal{U}_N), \quad (22)$$

which is equivalent to the following tensor-train representation:

$$\mathcal{Y}_c^k = \mathcal{U}_1 \times_{\frac{1}{3}} \dots \times_{\frac{1}{3}} \mathcal{U}_d \times_{\frac{1}{3}} X_c^k \times_{\frac{1}{2}} \mathcal{U}_{d+1} \times_{\frac{1}{3}} \dots \times_{\frac{1}{3}} \mathcal{U}_N. \quad (23)$$

This tensor-train formulation is graphically represented in Fig. 6 where the decomposition, i.e. \mathcal{X}_c^k , has two branches, thus we denote it as Two-way Tensor Train Decomposition (2WTT).

To maximize discriminability using 2WTT, an optimization scheme that alternates between the two sets of TT-subspaces can be utilized. This will reduce the dimensionality of the input by projecting it to a lower rank matrix. Computational complexity will then be reduced as the cost of computing scatter matrices and the number of matrix multiplications to find \mathcal{A}_n in (17) will decrease. We propose the procedure given in Algorithm 2 to implement this approach and refer to this approach of implementing TTDA as Two-way Tensor Train Discriminant Analysis (2WTTDA).

To determine the value of d in (22), we use a center of mass approach and find the d that minimizes $|\prod_{i=1}^d I_i - \prod_{j=d+1}^N I_j|$.

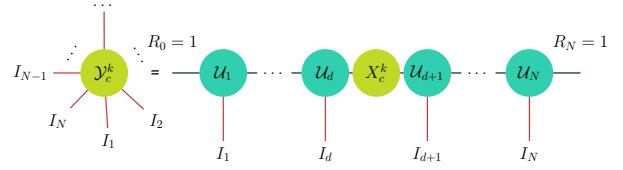


Fig. 6: Two-Way Tensor Train Decomposition (2WTT)

In this manner, the problem can be separated into two parts which have similar computational complexities.

Algorithm 2 Two-Way Tensor-Train Discriminant Analysis (2WTTDA)

Input: Input tensors $\mathcal{Y}_c^k \in \mathbb{R}^{I_1 \times I_2 \times \dots \times I_N}$ where $c \in \{1, \dots, C\}$ and $k \in \{1, \dots, K\}$, initial tensor factors $\mathcal{U}_n, n \in \{1, \dots, N\}$, $d, \lambda, R_1, \dots, R_N, MaxIter, LoopIter$

- Output:** $\mathcal{U}_n, n \in \{1, \dots, N\}$, and $X_c^k, \forall c, k$
- 1: **while** $iter < LoopIter$ **do**
 - 2: $\mathcal{Y}_L \leftarrow \mathcal{Y} \times_{d+1, \dots, N}^{2, \dots, N-d+1} (\mathcal{U}_{d+1} \times_{\frac{1}{3}} \dots \times_{\frac{1}{3}} \mathcal{U}_N)$.
 - 3: $[\mathcal{U}_i] \leftarrow TTDA(\mathcal{Y}_L, \lambda, R_i, MaxIter) \forall i \in \{1, \dots, d\}$.
 - 4: $\mathcal{Y}_R \leftarrow \mathcal{Y} \times_{1, \dots, d}^{2, \dots, d+1} (\mathcal{U}_1 \times_{\frac{1}{3}} \dots \times_{\frac{1}{3}} \mathcal{U}_d)$.
 - 5: $[\mathcal{U}_i] \leftarrow TTDA(\mathcal{Y}_R, \lambda, R_i, MaxIter) \forall i \in \{d+1, \dots, N\}$.
 - 6: $iter = iter + 1$.
 - 7: **end while**
 - 8: $\mathcal{X}_c^k \leftarrow \mathbf{L}(\mathcal{U}_1 \times_{\frac{1}{3}} \dots \times_{\frac{1}{3}} \mathcal{U}_d)^\top \mathbf{T}_d(\mathcal{Y}_c^k) \mathbf{R}(\mathcal{U}_{d+1} \times_{\frac{1}{3}} \dots \times_{\frac{1}{3}} \mathcal{U}_N)^\top$.
-

C. Three-way Tensor Train Discriminant Analysis (3WTTDA):

Elaborating on the idea of 2WTTDA, one can increase the number of modes of the projected samples which will increase the number of tensor factor sets, or equivalently the number of subspaces to be approximated using TT structure. For example, one might choose the number of modes of the projections as three, i.e. $\mathcal{X}_c^k \in \mathbb{R}^{R_{d_1} \times R_{d_2} \times \hat{R}_{d_2}}$, where $1 < d_1 < d_2 < N$. This model, named as Three-way Tensor Train Decomposition(3WTT) is given in (24) and represented graphically in Fig. 7.

$$\mathcal{Y}_c^k = \left(\left(\mathcal{X}_c^k \times_{\frac{1}{3}}^{N-d_2+2} (\mathcal{U}_{d_2+1} \times_{\frac{1}{3}} \dots \times_{\frac{1}{3}} \mathcal{U}_N) \right) \times_{\frac{1}{2}}^{d_2-d_1+2} (\mathcal{U}_{d_1+1} \times_{\frac{1}{3}} \dots \times_{\frac{1}{3}} \mathcal{U}_{d_2}) \right) \times_{\frac{1}{3}}^{d_1+2} (\mathcal{U}_1 \times_{\frac{1}{3}} \dots \times_{\frac{1}{3}} \mathcal{U}_{d_1}). \quad (24)$$

To maximize discriminability using 3WTT, one can utilize an iterative approach as in 2WTTDA, where input tensors are projected on all tensor factor sets except the set to be optimized, then apply TTDA to the projections. This procedure can be repeated until a convergence criterion is met or a number of iterations is reached. The values of d_1 and d_2 are calculated such that the product of dimensions I_i corresponding to each set is as close to $(\prod_{i=1}^N I_i)^{1/3}$ as possible. It is important to note that 3WTT will only be meaningful for tensors of order

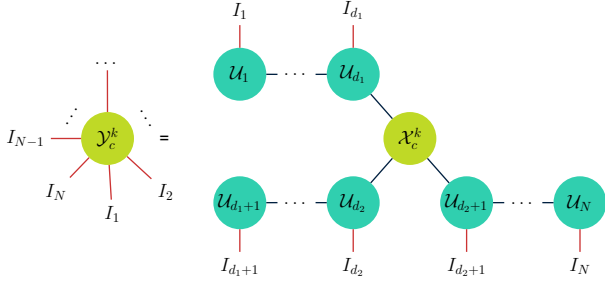


Fig. 7: Tensor Train Decomposition Three-Way. Note that the R s at the end of each branch disappear as they are equal to 1.

three or higher. When tensors are of order three, 3WTT is equivalent to Tucker Model.

D. Computational and Storage Complexity

In this section, we analyze the computational and storage complexities of the aforementioned algorithms.

Storage Complexity: Let $I_n = I, \forall n \in \{1, \dots, N\}$ and $R_l = r, \forall l \in \{2, \dots, N-1\}$. Assuming N is a multiple of both 2 and 3, total storage complexities are:

- $\mathcal{O}((N-1)r^2I + rI + rCK)$ for TT Decomposition, where $R_1 = 1, R_N = r$;
- $\mathcal{O}((N-2)r^2I + 2rI + r^2CK)$ for Two-Way TT Decomposition, where $R_1 = R_N = 1$;
- $\mathcal{O}((N-3)r^2I + 3rI + r^3CK)$ for Three-Way TT Decomposition, where $R_1 = R_{d_1} = R_N = 1$;
- $\mathcal{O}(NrI + r^NCK)$ for Tucker Decomposition, where $R_1 = R_N = r$.

TABLE I: Storage Complexities of Various Algorithms

$\mathcal{O}(\cdot)$	Subspace	Projection
TT	$(N-1)r^2I + rI$	rCK
2WTT	$(N-2)r^2I + 2rI$	r^2CK
3WTT	$(N-3)r^2I + 3rI$	r^3CK
TD	NrI	r^NCK

These results show that when the number of modes for the projected samples is increased, the storage cost increases exponentially for \mathcal{X}_c^k while the cost of storing \mathcal{U}_n s decreases quadratically. Using the above, one can easily find an optimal number of modes where the storage complexity is the lowest. Let the number of modes of \mathcal{X}_c^k be denoted by f . The storage complexity of the decomposition is then $\mathcal{O}((N-f)r^2I + frI + r^fCK)$. The optimal storage complexity is achieved by taking the derivative of the complexity in terms of f and equating it to zero. In this case, the optimal f is given by

$$\hat{f} = \text{round} \left(\log_r \left(\frac{r^2I - rI}{CK \ln(r)} \right) \right),$$

where $\text{round}(\cdot)$ is an operator that rounds to the closest positive integer.

Computational Complexity: For all the decompositions mentioned except DGTDA and LDA, the \mathcal{U}_n s and \mathcal{X}_c^k depend on each other which makes these decompositions iterative. The number of iterations will be denoted as t_c and t_t for

CMDA and TT-based methods, respectively. Also, for the sake of simplicity, we define $C_s = 2CK$. The total cost of finding \mathcal{U}_n s and $\mathcal{X}_c^k \forall n, c, k$, where $r \ll I$ is in the order of:

- $\mathcal{O} \left(I^N [(C_s + t_t r(r + N - 1))I^N + t_t r^4(I + r^2 I^{-1})] \right)$ for TTDA;
- $\mathcal{O} \left(r I^N \frac{C_s}{2} + 2I^{N/2} [(C_s + t_t r(r + N/2 - 1))I^{N/2} + t_t r^4 I + t_t r^6 I^{-1}] \right)$ for 2WTTDA;
- $\mathcal{O} \left(r I^N \frac{C_s}{2} + 3I^{N/3} [(C_s + t_t r(r + N/3 - 1))I^{N/3} + t_t r^4 I + t_t r^6 I^{-1}] \right)$ for 3WTTDA.

If convergence criterion is met with a small number of iterations, i.e. $t_t r(r + N/f - 1) \ll C_s$, and $I^{N/f} \gg r^6$ for all f , the reduced complexities are as given in Table II.

TABLE II: Computational complexities of various algorithms. The number of iterations to find the subspaces are denoted as t_c for CMDA and t_t for TT-based methods. $C_s = 2CK$. ($r \ll I$, $t_t r(r + N/f - 1) \ll C_s$, and $I^{N/f} \gg r^6$)

$\mathcal{O}(\cdot)$	Order of Complexity
LDA	$C_s I^{2N} + I^{3N}$
DGTDA	$3I^3 + NC_s I^{N+1}$
CMDA	$2t_c I^3 + t_c N^2 C_s I^N$
TTDA	$C_s I^{2N}$
2WTTDA	$(r/2 + 2)C_s I^N$
3WTTDA	$(rI^{N/3}/2 + 3)C_s I^{2N/3}$

We can see from Table II that with increasing number of branches, TT-based methods become more efficient if the algorithm converges in a few number of iterations. This is especially the case if the ranks of tensor factors are low as this reduces the dimensionalities of the optimal solutions and the search algorithm finds a solution to (19) faster. When this assumption holds true, the complexity is dominated by the formation of scatter matrices. Note that the ranks are assumed to be much lower than dimensionalities and number of modes is assumed to be sufficiently high. When these assumptions do not hold, the complexity of computing \mathcal{A}_n might be dominated by terms with higher power of r . This indicates that TT-based methods are more effective when the tensors have higher number of modes and when the TT-ranks of the tensor factors are low. DGTDA has an advantage over all other methods as the solution for each mode is not dependent on other methods and is not iterative. On the other hand, the solution of DGTDA is not optimal and there are no convergence guarantees except when the ranks and initial dimensions are equal to each other which is equivalent to k-NN with no dimensionality reduction.

IV. EXPERIMENTS

In order to evaluate the proposed methods, we conducted classification experiments on different image and video data sets and compared our methods with LDA, DGTDA and CMDA¹. The experiments were conducted on COIL-100, Weizmann Face, Cambridge datasets. For all data sets and all methods, classification accuracy with respect to both storage

¹Implemented using the open toolbox provided in https://github.com/laurafroelich/tensor_classification

cost and computational complexity is computed. The classification accuracy is evaluated using a 1-NN classifier. All experiments were repeated 10 times with random selection of the training and test sets and average classification accuracies are reported.

In the following experiments, the storage complexity is quantified as the ratio of the total number of elements in the tensor factors ($\mathcal{U}_n, \forall n$) and projections ($\mathcal{X}_c^k, \forall c, k$) of training data to the size of the original training data ($\mathcal{Y}_c^k, \forall c, k$). Computational complexity is quantified as the time it takes to learn the subspaces. The varying levels of storage cost are obtained by varying R_i s in the implementation of the tensor decomposition methods. Using varying levels of truncation parameter $\tau \in (0, 1]$, the singular values smaller than τ times the largest singular value are dropped. The remaining are used to determine ranks R_i for both TT-based and TD-based methods. For TT-based methods, the ranks are selected using TT-decomposition proposed in [22], while for TD-based methods truncated HOSVD was used.

In order to compute the run time, for TT-based methods, each set of tensor factors is optimized until the change in the normalized difference between consecutive tensor factors is less than 0.1 or 200 iterations is completed. After computing a branch, no further optimizations are done on that branch, i.e. cycle of iterations between sets is repeated only once. CMDA iteratively optimizes the subspaces for a given number of iterations (which is set to 20 to increase speed in our experiments) or until the change in the normalized difference between consecutive subspaces is less than 0.1. DGTDA does not iterate over the computed subspaces, thus is usually the fastest method.

λ for each experiment was selected using a validation set composed of all of the samples in the training set and one sample of each class from the test set. Utilizing a leave-one-out approach on this validation data, 5 random experiments were conducted. The optimal λ was selected as the value that gave the best average classification accuracy among a range of λ values from 0.1 to 1000 increasing in a logarithmic scale. The samples of test data that are used in validation were not used in testing again. CMDA does not utilize the λ parameter while DGTDA utilizes eigendecomposition to find λ [9].

A. COIL-100

The dataset consists of 7,200 RGB images of 100 objects of size 128×128 . Each object has 72 images, where each image corresponds to a different pose angle ranging from 0 to 360 degrees with increments of 5 degrees [25]. For our experiments, we downsampled grayscale images of all objects to 64×64 .

In the first experimental setting (Setting 1), each sample image was reshaped to create a tensor of size $8 \times 8 \times 8 \times 8$. Reshaping the inputs into higher order tensors is a common practice and was studied in various works [26], [22], [27], [14], [20]. 20 samples from each class were selected randomly as training data and the remaining samples were used for testing, i.e. $\mathcal{Y} \in \mathbb{R}^{8 \times 8 \times 8 \times 8 \times 20 \times 100}$. In this case, optimal storage complexity is achieved when $\hat{f} = 1$, i.e. the number

of modes of \mathcal{X}_c^k is 1, which means TTDA is the best in terms of storage complexity. However, computational complexity of TTDA makes it prohibitive. For this reason, we evaluated the classification accuracy for $f = 2$ (2WTTDA) and $f = 3$ (3WTTDA).

In Fig. 8, we can see that 3WTTDA is better in terms of both computational complexity and classification accuracy than all other algorithms. Although DGTDA has some advantage in computational complexity, the storage requirements and poor classification accuracy still makes 3WTTDA and 2WTTDA preferable. It can also be seen that the storage cost of 2WTTDA stops increasing after some point. The reason for this is that the TT-ranks of tensor factors are constrained to be smaller than the corresponding mode's input dimensions. Thus, the storage complexity advantage of the TT-based methods is apparent in this case.

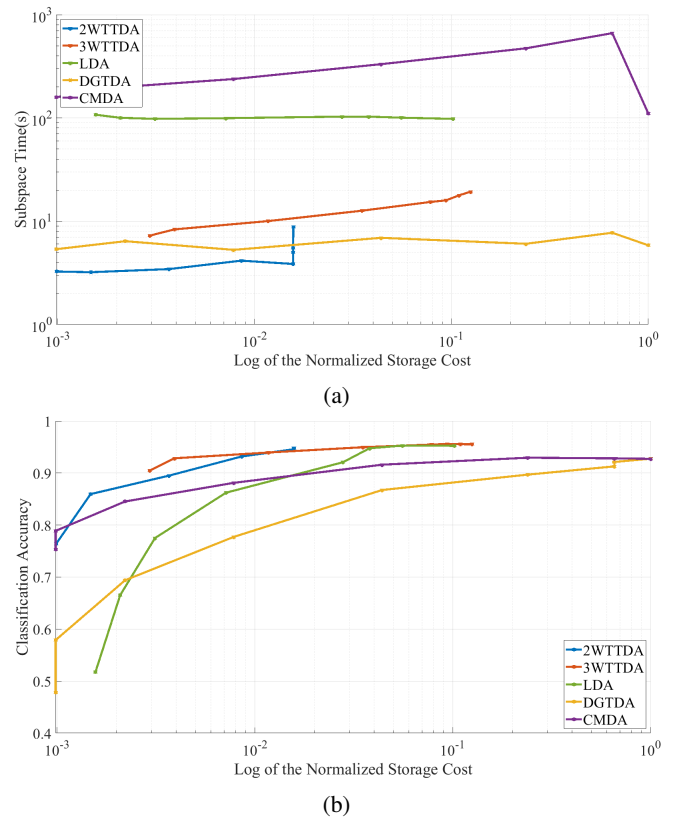


Fig. 8: Comparison of computation time, storage complexity and accuracy for Setting 1 of COIL-100 data: (a) Subspace computation time vs. storage complexity, (b) Classification accuracy vs. storage complexity for different methods.

In the next setting (Setting 2), for all 100 objects we created 9 tensors of size $64 \times 64 \times 8$ where each slice in the third mode is the image of the object with a 40 degree offset in pose angle from the former slice. In this experiment, 3WTTDA is equivalent to GTDA [11] since the number of modes of the input is the same as the number of modes of projections. 3 samples from each class were selected randomly as training data and the remaining samples were used for testing, i.e. $\mathcal{Y} \in \mathbb{R}^{64 \times 64 \times 8 \times 3 \times 100}$. In this example, LDA is not included in the comparisons due to extreme memory costs

of finding scatter matrices and eigendecomposition. Optimal storage complexity is achieved when the number of modes of \mathcal{X}_c^k is 1. The reason for this is that when the number of samples is too high compared to dimensions of the input tensor, total storage complexity is dominated by projected samples.

For this setting, we can see from Fig. 9 that TT-based methods provide the best classification accuracies along with reduced storage cost and computational complexity. Computational complexity of 2WTTDA increases after some point but even in that case, it is better than CMDA while still providing better accuracy.

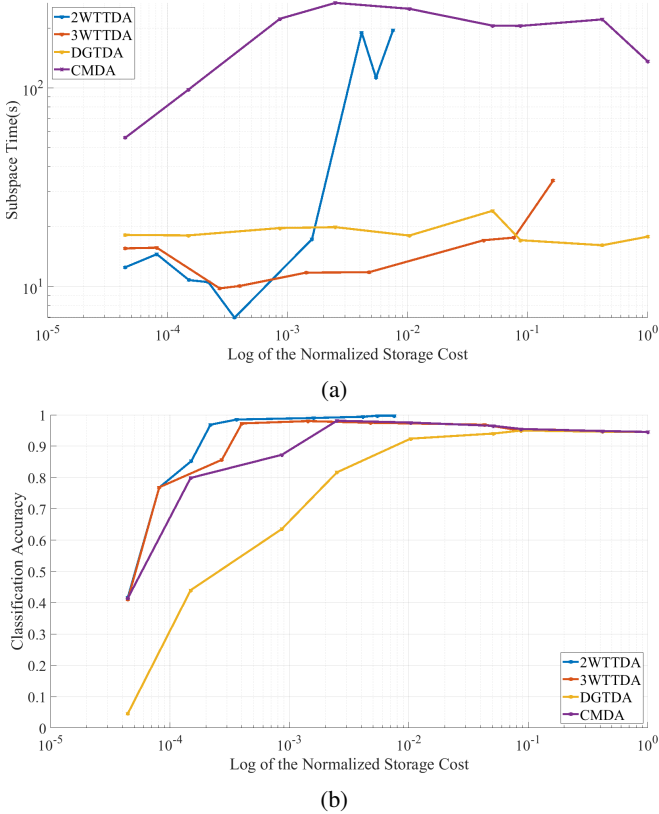


Fig. 9: Comparison of computation time, storage complexity and accuracy for Setting 2 of COIL-100 data: (a) Subspace computation time vs. storage complexity, (b) Classification accuracy vs. storage complexity for different methods.

B. Weizmann Face Database

The dataset includes RGB face images of size 512×352 belonging to 28 subjects taken from 5 viewpoints, under 3 illumination conditions, with 3 expressions [28]. For our experiments, each image was grayscaled, and downsampled to 64×44 . The images were then reshaped into 5-mode tensors of size $4 \times 4 \times 4 \times 4 \times 11$ as in [16]. For each experiment, 20 random tensors were selected to be training data and the remaining 25 samples were used in testing, i.e. $\mathcal{Y} \in \mathbb{R}^{4 \times 4 \times 4 \times 4 \times 11 \times 20 \times 28}$.

The results can be seen in Fig 10. In general, CMDA gives better results in terms of classification accuracy, but TT-based methods have better computational complexity and provide

similar or in some cases better accuracy when the ranks are sufficiently high. This is especially the case for 3WTTDA as computational complexity is always much better than CMDA. The best classification accuracy is provided by 3WTTDA as the storage cost increases. Note that the lower storage costs do not provide good results in terms of classification accuracy for any of the algorithms, thus making comparisons for these storage costs not very meaningful.

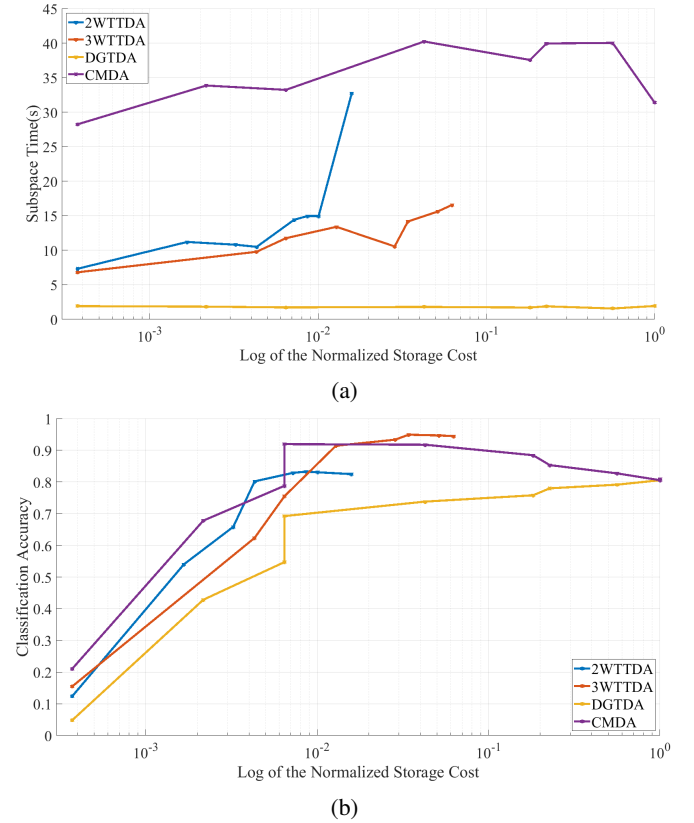


Fig. 10: Comparison of computation time, storage complexity and accuracy for Weizmann Dataset: (a) Subspace computation time vs. storage complexity, (b) Classification accuracy vs. storage complexity for different methods.

C. Cambridge Hand-Gesture Database

The data set consists of 900 image sequences of 9 gesture classes, which are combinations of 3 hand shapes and 3 motions. For each class, there are 100 image sequences generated by the combinations of 5 illuminations, 10 motions and 2 subjects [29]. Sequences consist of images of size 240×320 and sequence length varies. In our experiments, we used grayscaled versions of the sequences and we downsampled all sequences to length 30. We also included 2 subjects and 5 illuminations as the fourth mode. Thus, we have 10 samples for each of the 9 classes from which we randomly select 4 samples as the training set and the remaining 6 as test set, i.e. $\mathcal{Y} \in \mathbb{R}^{30 \times 40 \times 30 \times 10 \times 4 \times 9}$. For this dataset, optimal storage complexity is achieved when the number of modes of \mathcal{X}_c^k is 3 for low ranks and 2 for bigger ranks due to the small number

of samples compared to the dimensions of training samples \mathcal{Y}_c^k .

The results of the experiments can be seen in Fig. 11. It can be seen that the accuracy of both 2WTTDA and 3WTTDA are better than DGTDA and CMDA. Storage cost for TT-based methods are in general better than both Tucker-based methods and computational complexity is significantly better than CMDA when ranks are low, which is especially true for 3WTTDA. For 2WTTDA, the complexity gets worse after some point but the accuracy is still better compared to CMDA. The difference in computational complexity with DGTDA is not very significant for lower ranks, but even then, the accuracy is better than both Tucker-based methods.

storage complexity is also derived. It is important to note that as the number of modes in the projection tensor increases, computational complexity of the proposed structure improves while storage complexity is in most cases better than that of TD-based methods with same ranks. The number of branches of TT can only be increased when the number of modes of the input tensor is high, which becomes increasingly common with the advance of big data. Thus, the advantages of the proposed TT structures become more apparent when the data have a high number of modes.

While providing efficiency in terms of storage and computational costs, the proposed methods also show higher or similar classification accuracy compared to state-of-the-art methods such as CMDA. In future work, the convergence of the proposed structure can also be extended for unsupervised methods, dictionary learning, and subspace learning applications. The structure can also be optimized by permuting the modes in a way that the dimensions are better balanced than the original order.

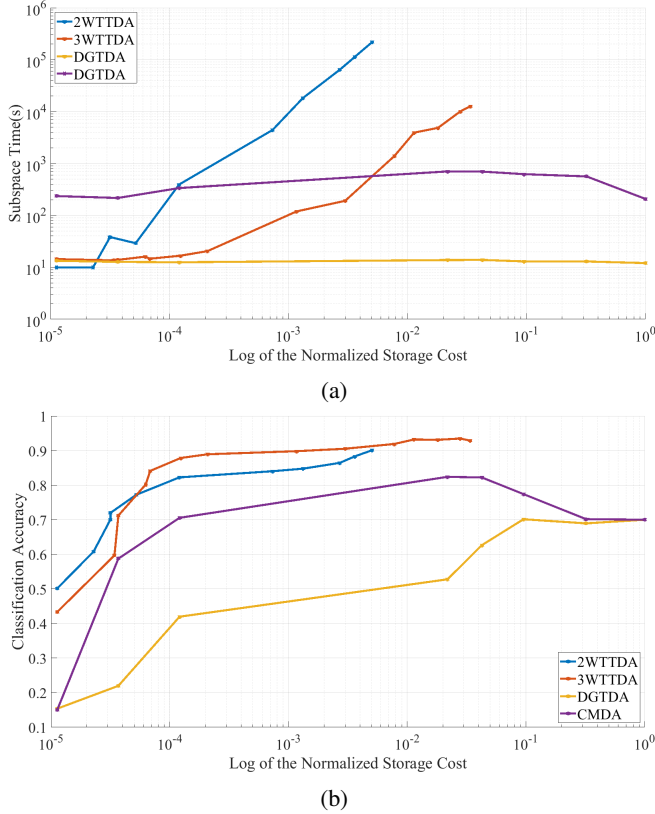


Fig. 11: Comparison of computation time, storage complexity and accuracy for Cambridge Hand-Gesture Dataset: (a) Subspace computation time vs. storage complexity, (b) Classification accuracy vs. storage complexity for different methods.

V. CONCLUSIONS

In this paper, we proposed a novel approach for tensor train based discriminant analysis for tensor object classification. Different rehapings of the tensor structure resulted in different ways to implement TT decomposition. This approach was used to define three different ways in which Tensor Network can be utilized. These methods were compared with the state-of-the-art TT-based discriminant analysis and LDA using several datasets. Theoretical analysis of storage complexity and computational complexity are provided. An optimal number of modes in the reshaping of TT structure for minimizing

REFERENCES

- [1] N. D. Sidiropoulos, L. De Lathauwer, X. Fu, K. Huang, E. E. Papalexakis, and C. Faloutsos, "Tensor decomposition for signal processing and machine learning," *IEEE Transactions on Signal Processing*, vol. 65, no. 13, pp. 3551–3582, 2017.
- [2] A. Cichocki, "Era of big data processing: A new approach via tensor networks and tensor decompositions," *arXiv preprint arXiv:1403.2048*, 2014.
- [3] T. G. Kolda and B. W. Bader, "Tensor decompositions and applications," *SIAM review*, vol. 51, no. 3, pp. 455–500, 2009.
- [4] R. Bro, "Parafac. tutorial and applications," *Chemometrics and Intelligent Laboratory Systems*, vol. 38, no. 2, pp. 149–171, 1997.
- [5] E. Acar and B. Yener, "Unsupervised multiway data analysis: A literature survey," *IEEE Transactions on Knowledge and Data Engineering*, vol. 21, no. 1, pp. 6–20, 2009.
- [6] L. De Lathauwer, B. De Moor, and J. Vandewalle, "A multilinear singular value decomposition," *SIAM journal on Matrix Analysis and Applications*, vol. 21, no. 4, pp. 1253–1278, 2000.
- [7] —, "On the best rank-1 and rank-(r_1, r_2, \dots, r_n) approximation of higher-order tensors," *SIAM journal on Matrix Analysis and Applications*, vol. 21, no. 4, pp. 1324–1342, 2000.
- [8] A. Cichocki, D. Mandic, L. De Lathauwer, G. Zhou, Q. Zhao, C. Caiafa, and H. A. Phan, "Tensor decompositions for signal processing applications: From two-way to multiway component analysis," *IEEE Signal Processing Magazine*, vol. 32, no. 2, pp. 145–163, 2015.
- [9] Q. Li and D. Schonfeld, "Multilinear discriminant analysis for higher-order tensor data classification," *IEEE Transactions on Pattern Analysis and Machine Intelligence*, vol. 36, no. 12, pp. 2524–2537, 2014.
- [10] S. Yan, D. Xu, Q. Yang, L. Zhang, X. Tang, and H.-J. Zhang, "Discriminant analysis with tensor representation," in *Computer Vision and Pattern Recognition, 2005. CVPR 2005. IEEE Computer Society Conference on*, vol. 1. IEEE, 2005, pp. 526–532.
- [11] D. Tao, X. Li, X. Wu, and S. J. Maybank, "General tensor discriminant analysis and gabor features for gait recognition," *IEEE Transactions on Pattern Analysis and Machine Intelligence*, vol. 29, no. 10, 2007.
- [12] H. Wang, S. Yan, T. S. Huang, and X. Tang, "A convergent solution to tensor subspace learning," in *IJCAI, 2007*, pp. 629–634.
- [13] H. Lu, K. N. Plataniotis, and A. N. Venetsanopoulos, "MPCA: Multilinear principal component analysis of tensor objects," *IEEE Transactions on Neural Networks*, vol. 19, no. 1, pp. 18–39, 2008.
- [14] A. Cichocki, A.-H. Phan, Q. Zhao, N. Lee, I. Oseledets, M. Sugiyama, D. P. Mandic *et al.*, "Tensor networks for dimensionality reduction and large-scale optimization: Part 2 applications and future perspectives," *Foundations and Trends® in Machine Learning*, vol. 9, no. 6, pp. 431–673, 2017.
- [15] J. A. Bengua, P. N. Ho, H. D. Tuan, and M. N. Do, "Matrix product state for higher-order tensor compression and classification," *IEEE Transactions on Signal Processing*, vol. 65, no. 15, pp. 4019–4030, 2017.
- [16] W. Wang, V. Aggarwal, and S. Aeron, "Tensor train neighborhood preserving embedding," *IEEE Transactions on Signal Processing*, vol. 66, no. 10, pp. 2724–2732, 2018.
- [17] A. Novikov, D. Podoprikin, A. Osokin, and D. P. Vetrov, "Tensorizing neural networks," in *Advances in Neural Information Processing Systems*, 2015, pp. 442–450.
- [18] A. Cichocki, N. Lee, I. Oseledets, A.-H. Phan, Q. Zhao, D. P. Mandic *et al.*, "Tensor networks for dimensionality reduction and large-scale optimization: Part 1 low-rank tensor decompositions," *Foundations and Trends® in Machine Learning*, vol. 9, no. 4-5, pp. 249–429, 2016.
- [19] W. Wang, V. Aggarwal, and S. Aeron, "Efficient low rank tensor ring completion," in *Proceedings of the IEEE International Conference on Computer Vision*, 2017, pp. 5697–5705.
- [20] J. A. Bengua, H. N. Phien, H. D. Tuan, and M. N. Do, "Efficient tensor completion for color image and video recovery: Low-rank tensor train," *IEEE Transactions on Image Processing*, vol. 26, no. 5, pp. 2466–2479, 2017.
- [21] S. Holtz, T. Rohwedder, and R. Schneider, "On manifolds of tensors of fixed tt-rank," *Numerische Mathematik*, vol. 120, no. 4, pp. 701–731, 2012.
- [22] I. V. Oseledets, "Tensor-train decomposition," *SIAM Journal on Scientific Computing*, vol. 33, no. 5, pp. 2295–2317, 2011.
- [23] Z. Wen and W. Yin, "A feasible method for optimization with orthogonality constraints," *Mathematical Programming*, vol. 142, no. 1-2, pp. 397–434, 2013.
- [24] J. Ye, R. Janardan, and Q. Li, "Two-dimensional linear discriminant analysis," in *Advances in Neural Information Processing Systems*, 2005, pp. 1569–1576.
- [25] S. A. Nene, S. K. Nayar, and H. Murase, "Columbia object image library (coil-100)."
- [26] B. N. Khoromskij, "O (dlog n)-quantics approximation of n-d tensors in high-dimensional numerical modeling," *Constructive Approximation*, vol. 34, no. 2, pp. 257–280, 2011.
- [27] Q. Zhao, G. Zhou, S. Xie, L. Zhang, and A. Cichocki, "Tensor ring decomposition," *arXiv preprint arXiv:1606.05535*, 2016.
- [28] "Weizmann facebase," <http://www.wisdom.weizmann.ac.il/~vision/FaceBase/>.
- [29] T.-K. Kim, S.-F. Wong, and R. Cipolla, "Tensor canonical correlation analysis for action classification," in *2007 IEEE Conference on Computer Vision and Pattern Recognition*. IEEE, 2007, pp. 1–8.